A Vertical Cavity Longwave Infrared SiGe/Si Photodetector Using a Buried Silicide Mirror

R T Carline, D A O Hope, V Nayar, D J Robbins and M B Stanaway

Defence Evaluation and Research Agency
Malvern, WR14 3PS UK

Abstract

We describe the fabrication, modelling and performance of a resonant cavity detector using epitaxial p-type SiGe/Si quantum wells grown over a high reflectance tungsten silicide layer. The device operates in the 8-12μm band in normal incidence and has a black body responsivity comparable to current n-GaAs/AlGaAs detectors at ~1V, making it suitable for integration in a monolithic Si-based focal plane array. Ways to improve the design are discussed.

Introduction

Staring focal plane arrays (FPAs) for thermal imaging are generally based on Si readout circuits which are combined with 2-dimensional (2D) detector arrays. In the 3-5μm atmospheric window the highest performance systems require cryogenic cooling and use hybridised InSb or HgCdTe photon detector arrays, while large FPAs (maximising pixel numbers and field-of-view) use monolithically integrated Si circuits and PtSi Schottky barrier detectors. At the longer wavelength (8-12μm) atmospheric window hybridised n-type GaAs/AlGaAs quantum well infrared photodetector (QWIP) arrays (2) deliver the best performance. The absorption in these QWIPs is due to intersubband transitions with low intrinsic quantum efficiency (QE) compared with direct gap HgCdTe alloys, but the relative maturity of GaAs/AlGaAs technology has allowed fabrication of large, uniform 2D arrays. The use of IrSi Schottky barriers or single heterojunction p-SiGe/Si detectors (3) to make monolithic FPAs in the 8-12μm band has not proved commercially viable due to their low QE and detectivity in this wavelength range.

The fabrication of n-GaAs/AlGaAs QWIPs is complicated by the need for a special structure on each pixel to scatter the incident light in a direction parallel to the plane of the FPA to allow intersubband absorption. In order to minimise optical cross-talk between pixels and to increase the effective path length by trapping light within a pixel, the GaAs substrate wafer in the hybridised QWIP array is usually polished to a few microns thickness, increasing fabrication costs.

P-type QWIPs differ from these well-known n-type devices in absorbing light propagating normal to the plane of the detector array (3). In this paper we describe a new device using a p-SiGe/Si QWIP grown on a bonded silicon-on-insulator wafer incorporating a buried WSi_2 layer as a broad-band reflector to form a vertical resonant cavity structure. Normally-incident radiation at the resonance wavelength creates a standing optical wave in the cavity which increases the QE compared with a similar QWIP on a bulk Si substrate. This geometry achieves increased absorption and low optical cross-talk without the need for expensive wafer thinning.

Experimental Methods

The final device is shown schematically in Fig. 1. The substrate was a bonded wafer fabricated by BCO Technologies, Northern Ireland. A 0.3μm thick tungsten silicide ($WSi_{2.7}$) layer was deposited on a Si wafer, using industry-standard chemical vapour deposition (CVD), followed by a 1μm thick deposited oxide layer. The silicided wafer was bonded to a handle wafer and then thinned to produce a silicon-silicide-on-insulator (S^2OI) substrate (4).

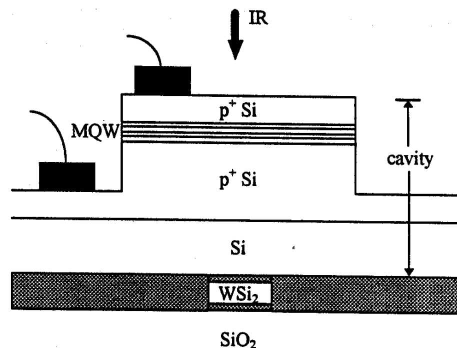

Figure 1. Schematic cross-section of the resonant cavity device incorporating a 16 period SiGe/Si QWIP. The epitaxy begins at the p^+Si/Si interface.

0-7803-4100-7/97/$10.00 © 1997 BCC

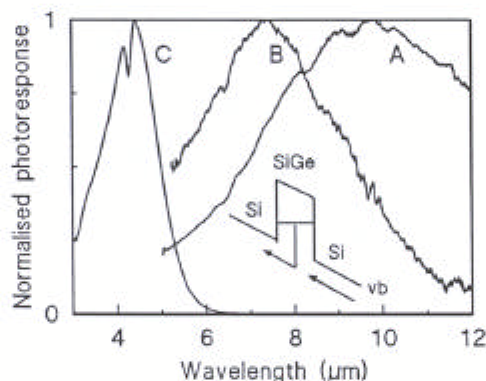

Fig. 2. Relative normal incidence photoconductivity spectra for 30 period p-SiGe/Si QWIPs on bulk Si substrates. The Ge fraction in the SiGe alloys increases from A to C. The inset illustrates photoexcitation of holes.

The 16-period, p-$Si_{0.86}Ge_{0.14}$ /Si resonant cavity QWIP was grown epitaxially on this S^2OI substrate at 650°C by low pressure CVD using $H_2/SiH_4/GeH_4$ mixtures at a total pressure of 20 Pa. The 16 alloy quantum wells were nominally 5nm thick, each doped p-type with a sheet concentration ~ 1.5e12cm^{-2} using B_2H_6, and the nominally-undoped Si barrier layers were 55nm thick. The p^+-Si contact layers were doped at ~3e18cm^{-3}. A 1mm diameter photoconductive detector was fabricated by wet etching to form an unpassivated mesa-isolated structure, followed by deposition, patterning and alloying of Al to form ohmic contacts as illustrated in Fig. 1. A 30 period p-SiGe/Si QWIP with similar composition was fabricated on a bulk p^+-Si wafer as a non-resonant reference device in which the incident radiation was attenuated after a single optical pass through the QWIP region.

The normal incidence reflectances of the bonded substrate and the resonant cavity QWIP were measured using a Perkin-Elmer 983G spectrophotometer with gold as 100% reflectance standard. Normal incidence, black body responsivities were measured at ~25K by flood illumination of the sample in a cryostat with radiation from a calibrated 500K oven source; the incident power flux was checked by replacing the sample in the cryostat with a calibrated pyroelectric detector. Spectral responsivities were obtained by integration over the photoconductivity spectrum measured relative to a pyroelectric detector using the method described in (5).

Optical Properties

Absorption in the heavily-doped p-SiGe QWs is dominated by direct inter-valence-band transitions broadened by

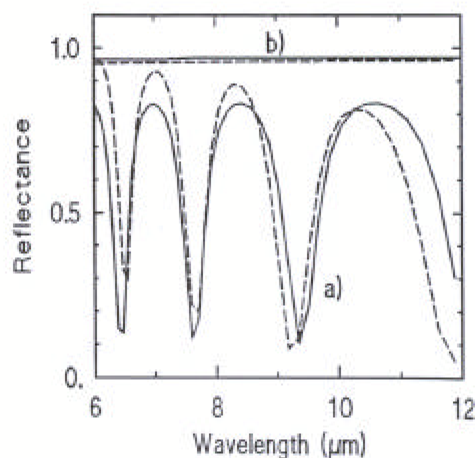

Fig. 3. Reflectance spectra at 293K, measured (solid line) and simulated (dashed line) for a) the resonant cavity device and b) the WSi_2 reflector in a S^2OI substrate after removal of the Si overlayer. Unity reflectance represents a Au standard.

impurity scattering, giving a Drude-like dispersion (6). The energy dependence of responsivity is determined by the dispersion of both the absorption intensity and the probability that photo-excited holes escape from the QW into the Si barrier layer, contributing to the photocurrent. The spectral responsivity for non-resonant p-SiGe/Si QWIPs on bulk Si substrates is quite broad, and can be tailored by varying alloy composition and QW width (Fig 2). The QW composition for this work was chosen to give a peak responsivity near 9μm in a non-resonant device. In order to achieve resonantly-enhanced absorption at that wavelength, the cavity in Fig. 1 was designed to be 5.9μm thick to generate a standing optical wave for incident 9μm radiation.

The specification was checked after growth of the QWIP on the S^2OI wafer by measurement of the device reflectance and comparison with optical models. The reflectance spectrum was simulated using Fresnel's equations with room temperature refractive indices representing the individual layers and assuming abrupt interfaces. The buried silicide mirror was represented as a W/Si mixture, the reflectance of this simulated layer giving good agreement with the measured reflectance of a real silicide layer after removal of the overlying Si (Fig. 3). The top reflector is formed by the Si/ ambient interface. The cavity thickness was varied to fit the simulated reflectance to the measured spectrum. The good agreement in Fig. 3 was obtained assuming a cavity thickness of 6μm, close to the original design value of 5.9μm. The minima in the reflectance spectrum occur at resonance wavelengths where standing optical waves are generated in the cavity structure.

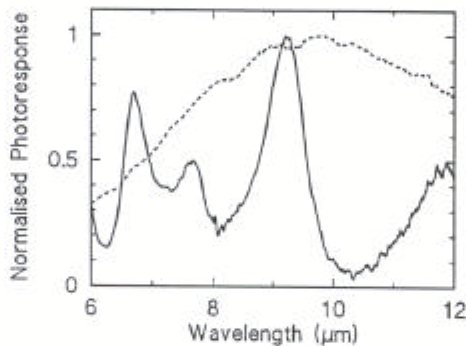

Fig. 4: Relative photoresponse spectra for the resonant cavity QWIP (solid line) and the non-resonant reference QWIP (dashed line) at 20K.

Detector Properties

A. Spectral Responsivity

The spectral responsivities of the non-resonant device on bulk Si and the resonant cavity device on the S^2OI wafer are compared in Fig 4. The relatively broad spectrum of the non-resonant QWIP peaks between 9-10μm, with a cut-off wavelength ~13μm; this is the characteristic response for the 5nm thick $Si_{0.86}Ge_{0.14}$ QWs. The responsivity of the cavity device shows strong enhancement at the resonance wavelengths determined from the reflectance spectrum in Fig 3, with the most intense peak at 9.2μm. The square of

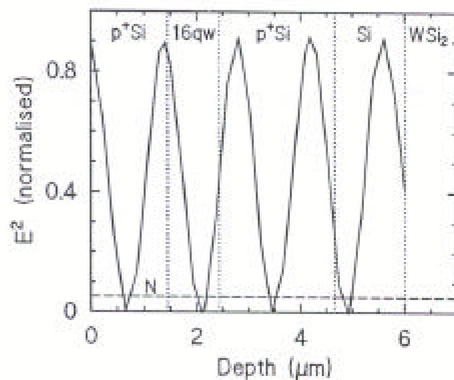

Fig. 5. Relative magnitudes of the square of the optical electric field strength through various regions of the resonant cavity device with unit incident field strength at 9.2μm. The dashed line 'N' represents absorption at this wavelength in the non-resonant device. Peak absorption intensity is ~16X higher in the standing wave of the resonant cavity device

the calculated optical electric field strength at this resonance is shown as a function of position in the cavity in Fig. 5, assuming unit incident field strength. This quantity is proportional to the absorption intensity. The absolute peak responsivities in Fig 4, using similar bias fields across the 30 period non-resonant QWIP and the 16 period resonant devices, are 20mA/W (resonant) at 0.2V and 2.5mA/W (non-resonant) at 0.5V bias. This 8X enhancement in responsivity at 9-10μm for the resonant device is less than the 16X increase in peak absorption intensity predicted in Fig 5 because the 16 period QWIP structure spans regions of high and low intensity in the standing wave.

B. Dark Current

Dark currents for the non-resonant and resonant QWIPs were measured at different temperatures with the devices totally enclosed in a cooled package. The temperature dependences are compared in Fig. 6, using bias voltages which generate similar electric fields across the devices. The higher-temperature dark currents due to thermally-activated emission from the QWs, and the low temperature leakage currents, are similar for the two unpassivated devices, demonstrating high quality epitaxy on the S^2OI wafer.

C. Black Body Responsivity

The bias-dependence of the 500K black body responsivities for the non-resonant and resonant SiGe/Si QWIPs measured in normal incidence are shown in Fig. 7. Comparing voltages at which the bias fields across the active regions of the two devices are similar, the black body responsivity of the 16 period resonant QWIP at 0.5V (9.1mA/W) is more than 5X higher than that of the 30 period non-resonant QWIP at 1V (1.6mA/W); in the latter the radiation makes only a single pass through the QWIP before absorption in the substrate.

The corresponding black body responsivities for two 50 period n-GaAs/AlGaAs QWIPs are also shown in Fig. 7. Curve 7c is the responsivity of a discrete GaAs QWIP using a bound-continuum transition with a 12.4μm cut-off (7). The data were taken in this laboratory in a multi-pass waveguide with 45° angle of incidence using the same measurement equipment as for the normal incidence p-SiGe/Si devices; in the waveguide geometry the radiation effectively makes a double pass through the active region. Curve 7d is the black body responsivity derived from published data on a FPA using a bound-bound n-GaAs/AlGaAs QWIP with 8.9μm cut-off; this device is hybridised on a Si readout circuit and operates in normal incidence using a scattering surface layer (8). The black body responsivity was derived from the published responsivity spectrum and the power spectrum of the 500K black body source, using methods described in (5).

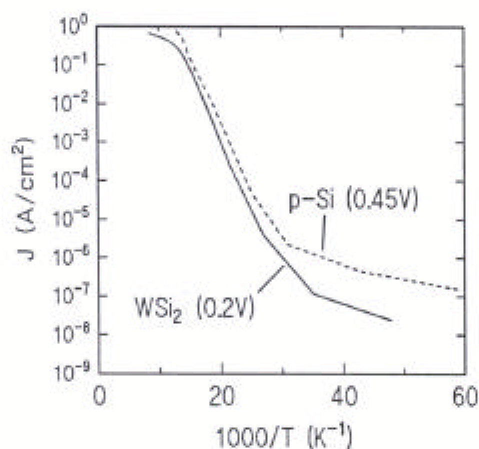

Fig. 6. Temperature-dependence of dark current densities for the resonant (WSi_2, 16 period) and non-resonant (p-Si, 30 period) QWIPs. The bias fields across the active QW regions are similar. The thermal activation energies are 80meV (resonant) and 75meV (non-resonant).

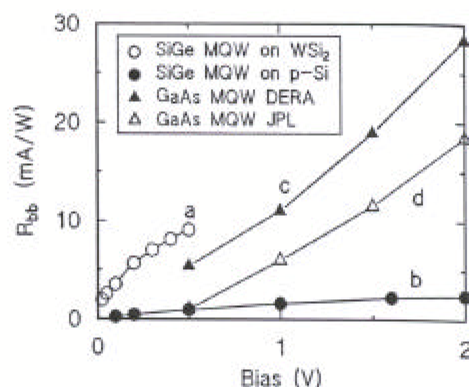

Fig. 7. Comparison of external 500K black body responsivities. (a) 16 period resonant SiGe/Si QWIP; (b) 30 period non-resonant SiGe/Si reference; (c) 50 period bound-continuum n-GaAs/AlGaAs QWIP in a waveguide; (d) 50 period bound-bound n-GaAs/AlGaAs QWIP used in a 256x256 FPA operating at 1V bias.

Discussion

At bias voltages up to ~1V, as used in a FPA, the normal incidence black body responsivity of the resonant p-SiGe/Si QWIP on the S^2OI substrate is similar to that of the n-GaAs/AlGaAs devices in Fig. 7. There are several ways in which the performance of this resonant SiGe/Si device might be improved. First, the thermal dark current could be reduced using a QWIP structure with a cut-off wavelength shorter than the 13μm used in this work; this would produce only a small reduction of peak responsivity in the resonant cavity. Secondly, the low temperature leakage currents could be reduced by suitable passivation of the mesa walls. Thirdly, the efficiency of coupling to the incident radiation could be increased by reducing the number of QWs in the device and positioning this smaller number near a maximum in the optical electric field (9). The photoconductive gain is inversely proportional to the number of QWs in the QWIP, and removing the wells which lie at a region of low field strength in the cavity standing wave in Fig. 5, and which therefore contribute little to the absorption in the present device, would increase the photocurrent almost in proportion to the increase in gain.

In conclusion, we have shown that the normal incidence responsivity for a p-SiGe/Si QWIP incorporated in a vertical resonant cavity device using a buried silicide reflector is comparable to that of III-V QWIPs already used in FPA cameras for long wavelength imaging. The new device offers a route to large area monolithic FPAs for the 8-12μm band, where the QWIP is integrated by epitaxial growth on the Si readout circuit. An integrated FPA of this kind would be less expensive to fabricate than n-GaAs/AlGaAs FPAs which require hybridisation to a Si circuit and subsequent thinning to achieve high QE and low cross-talk, and would also avoid problems associated with differential contraction on cooling. The high reflectance of the silicide layer over the whole long wavelength band will allow tailoring of the QWIP composition and cavity thickness to optimise the peak response wavelength and to maximise the detectivity.

References

(1) A. Rogalski, "New trends in semiconductor infrared detectors", *Optical Eng.*, vol. 33, p. 1395, 1994.

(2) B.F. Levine, "Quantum well infrared photodetectors", *J. Appl. Phys*, vol. 74, p.R1, 1993.

(3) B-Y. Tsaur, C.K.Chen, and S.A.Marino, "Heterojunction GeSi/Si infrared detectors and focal plane arrays", *Optical Eng.*, vol.33, p.72, 1994.

(4) R.Wilson, C.Quinn, B.McDonnell, S.Blackstone, and K.Yallup, "Bonded and trenched SOI with buried silicide layers", in *Electrochem. Soc. Proc.*, Vol. 95-7, C.E.Hunt Ed., Pennington, NJ, 1995, p. 535.

(5) A.Zussman, B.F.Levine, J.M.Kuo, and J.de Jong, "Extended long-wavelength GaAs/AlGaAs quantum-well infrared photodetectors", *J. Appl. Phys.*, vol.70, p.5101, 1991.

(6) D.J.Robbins, M.B.Stanaway, W.Y.Leong, R.T.Carline, and N.T.Gordon, "Absorption in SiGe quantum well detectors", *Appl. Phys. Lett.*, vol 66, p.1512, 1995.

(7) M.J.Kane, S.Millidge, M.T.Emeny, D.Lee, D.R.P.Guy, and C.R.Whitehouse, "Performance trade offs in the quantum well infrared detector", in *Intersubband Transitions in Quantum Wells*, E.Rosencher Ed., Plenum Press, New York, 1992, p.31.

(8) S.D.Gunapala, J.K.Liu, J.S.Park, M.Sundaram, C.A.Shott, T. Hoelter, T-L.Lin, S.T.Massie, P.D.Maker, R.E. Muller, and G.Sarusi, "9μm cutoff 256x256 GaAs/AlGaAs QWIP hand-held camera", *IEEE Trans. Electron Dev.*, vol. 44, p.51, 1997

(9) R.T.Carline, D.A.Hope, M.B.Stanaway, and D.J.Robbins, "Controlled growth of long wavelength SiGe/Si quantum well resonant cavity photodetectors", *Proc. SPIE*, Vol. 3007, D. C. Houghton and B Jalali Eds., Bellingham, Washington, 1997, p. 81.